

Estimating State of Charge for xEV batteries using 1D Convolutional Neural Networks and Transfer Learning

Arnab Bhattacharjee, Ashu Verma, *Senior Member, IEEE*, Sukumar Mishra, *Senior Member, IEEE*, Tapan K. Saha, *Fellow, IEEE*

Abstract—A state of charge estimator is an essential component of battery management systems used in Electric Vehicles. In the recent years deep learning algorithms have fared well as accurate and reliable state of charge estimators, owing to their high accuracy of estimation under noisy conditions and the relative ease with which they can process large amount of data. However, deep learning algorithms are extremely task specific and need to be retrained when the battery data distribution changes. This paper proposes a novel state of charge estimation algorithm consisting of one dimensional convolutional neural networks and also introduces a transfer learning framework for improving generalization across different battery data distributions. The proposed method fares well in terms of estimation accuracy, learning speed and generalization capability.

Index Terms—State of Charge Estimation, 1D CNN, Time series analysis, Electric Vehicles, Transfer Learning.

I. INTRODUCTION

ELectric vehicles (EVs) are likely to face an increasing demand as the green alternative to conventional fuel powered automobiles owing to their high efficiency, lower carbon footprint, usability as a portable storage element for electrical energy and the decreasing cost and size of batteries with high energy density. Li-ion batteries (LiBs) of various specifications and types are one of the most common sources of power used for electric vehicles, owing to their high energy density, low memory effects, high power to weight ratios and many such favorable properties. However, the use of batteries as the source of power for electric vehicles poses a very unique problem, one that their fuel powered counterparts never came across. Unlike a simple fuel gauge which could measure the amount of fuel remaining in a conventional IC engine powered vehicle, no instrument can directly measure or observe a similar quantity for the battery driven EVs. Hence the estimation of such a quantity is deemed essential for the evolution of EVs.

The state of charge or SoC is one such quantity which provides the information about the remaining amount of charge

Arnab Bhattacharjee is enrolled as a Ph.D. student in Electrical Engineering at the University of Queensland-IIT Delhi Academy of Research. email: Arnab.Bhattacharjee@uqidar.iitd.ac.in

Ashu Verma is associated with the Centre for Energy Studies, Indian Institute of Technology, Delhi, India, 110016. email: averma@ces.iitd.ac.in

Sukumar Mishra is associated with the Electrical Engineering Department, Indian Institute of Technology, Delhi, India, 110016. email: sukumar@ee.iitd.ac.in

Tapan K Saha is at the School of Information Technology and Electrical Engineering in the University of Queensland, Brisbane, Australia. email: saha@itee.uq.edu.au

in a battery as a ratio to its nominal capacity. SoC estimation is of paramount importance ([6]) owing to its applications in range estimation of an EV, initial charge estimation for charging operations, energy balancing operation amongst cells of a battery, demand response, Vehicle to vehicle (V2V) energy transfer scenarios and so on. Over the years, a wide range of battery state of charge estimators have been proposed in the literature and those can be broadly categorized into four types: lookup table method, ampere hour integral method, model based estimation method and model free estimation method.

The most basic forms of SOC estimators are based on a lookup table approach. A lookup table is built by identifying a relation between the SOC and some other measurable battery parameters like Open circuit voltage (OCV) or the AC impedance. During battery operation, the value of the measurable parameter is obtained and the SOC is looked up from a table ([1],[4]). Such methods are not scalable and only provide highly approximate values of SOC. Moreover, the observable battery parameters that are mostly used for the look up table correspond to battery static characteristics like OCV. Thus in order to measure these parameters, the battery needs to be put at rest for a long time to reach steady state.

If the initial SOC is known and the current can be measured precisely, the amount of charge lost or gained by the battery can be calculated by simply integrating the current over the time of battery operation. This simple approach known as the ampere hour integral method requires that the initial SOC is known and that the error or disturbances in current measurement is negligible. Also the total charge capacity of the battery needs to be re-calibrated with time owing to battery aging effects. This method is suitable for laboratory applications [6].

Model based estimation techniques use a mathematical model of the battery to form their state equations. Following this, adaptive filters and non linear estimation algorithms can be used to determine or estimate the internal states of the battery. Various non linear state estimation algorithms and filters have been used in literature for SOC estimation. Kalman filters and its various types have been widely used across literature for SOC estimation(([2],[7],[8],[11]) owing to their robustness, accuracy of estimation and ease of implementation. The estimation accuracy of these model based estimators heavily depend on the goodness of the battery models on which they are built. These models, however, are almost always based on some underlying simplifying assumptions

necessary to make them tractable and thus may fail to account for certain processes contributing to changes in the battery internal states.

In situations where the entire mathematical model of the battery is unknown or fails to account for the uncertainties in the system, model free approaches are the most preferred. As the name suggests these methods use non linear functions to adaptively identify the battery model from the observable parameter values and hence are capable of estimating the internal states of the battery directly from data. They are robust to noise, provide low values of estimation error and are highly scalable and easily deployable.

Machine learning and especially deep learning models are an important class of algorithms that can be used for data driven model free estimation purposes. Different types of neural networks have been used previously in literature for the purpose of SOC estimation. [3] used fuzzy neural networks and learning controllers for estimation purposes. A feed forward neural network was used for SOC estimation in [13], [14] and a backtracking search algorithm was employed for hyperparameter tuning in [14]. In [9], a robust sliding mode observer was used for the estimation purpose and an RBF neural network was used for adaptively developing an upper bound on the uncertainties.

Taking into consideration the temporal nature of battery observable data, numerous papers have come up where different forms of Recurrent Neural Networks have been proposed for SOC Estimation. [10] used dynamically driven RNNs for online estimation of SOC. [12] used Long Short Term Memory (LSTM) unit networks for SOC estimation. [16] used a hybrid Variable Auto-Regressive Moving Average(VARMA)- LSTM combination in order to separately estimate the linear and non linear components of current in order to estimate SOC. [17], [20] used Gated Recurrent Unit (GRU) networks for estimation purposes.

In recent times, the application of Convolutional Neural Networks (CNNs) for time series data analysis has been widely explored. But as far as our knowledge goes, the use of CNNs in a standalone fashion for SOC estimation has not been previously observed in literature. In [18], the authors use a hybrid CNN-LSTM network to estimate SOC where the spatial features from current input are extracted using the CNN while the temporal features from past inputs are extracted using the LSTM network.

Machine learning algorithms, although preferred for their accuracy in estimation, suffer from the limitation of being task specific. Transfer Learning deals with a class of algorithms which aim at solving the aforementioned problem. [19] used transfer learning for improving the generalization capability of their LSTM based SOC estimator. However, they used very shallow networks leading to high estimation errors.

This paper proposes a model free SoC estimation technique based on a deep wide one dimensional(1D) CNN. The width in the CNN allows for the identification of long and short term trends in the same time series data. Moreover, to ensure that the developed models are generalizable across data from different battery manufacturers, a transfer learning framework is proposed.

The key claims of this paper are highlighted below:

- 1) The 1D CNN based SOC estimator performs better than or at least at par with the existing state of art SoC estimators in terms of estimation error.
- 2) The time of offline training required before deploying the proposed model is lesser than the existing state of art machine learning based SoC estimators. The time further decreases when transfer learning is used.
- 3) By transferring learned weights of a model trained on a source battery dataset for training an identical model on a target battery dataset, using the transfer learning framework proposed in this paper, faster training is achieved and the estimation accuracy is found to be comparable to a model trained without using transfer learning.

The rest of the paper is organised in the following manner. Section II consists of a brief description of the SOC estimation problem formulation and introductions to the convolutional neural network and transfer learning algorithms used in the paper. The datasets are elaborated in section III. Section IV consists a description of the experimental setup and section V contains the experimental results and inferences. The paper is concluded in section VI.

II. PROPOSED METHOD

A. Problem Statement

The problem of estimating the state of charge of a battery is modelled as a time series analysis problem. The SOC at timestep k is a function of the observed battery parameters, i.e., the current, voltage and the battery temperature, measured till the timestep k . Here, we first model the SOC in the following way:

$$\widehat{SOC}_k = f(\phi_k, \phi_{k-1}, \dots, \phi_1) \quad (1)$$

where, $\phi_k = [V_k, I_k, T_k]^T$ and $k = 1, \dots, t_{end}$

where V_k , I_k and T_k are the voltage, current and temperature values measured at timestep k , t_{end} is the final timestep and f is a non linear mapping from the feature space to the label space.

The above functional model, however, poses a number of difficulties. Firstly, with a varying value of k , we would have to vary the input size or dimensions of the data driven estimator which can lead to difficulties during training. Secondly, as the value of k increases we need to increase the capacity of the data driven estimator model, as well, for obtaining good training dynamics. Keeping this in mind, we propose to model the SOC at the k -th timestep as a function of the observed battery parameters ranging from k to $k - t_w$ timestep, i.e., we take into account a fixed range of historical data to predict the current label. The time horizon/ range/ window, t_w , is kept fixed throughout the training and testing process and can be treated as a hyperparameter. Now the modified SOC model will look like this:

$$\widehat{SOC}_k = f_\theta(\phi_k, \phi_{k-1}, \dots, \phi_{k-t_w+1}) \forall k \geq t_w \geq 0 \quad (2)$$

with the symbols holding their usual meaning.

With this functional model, we need to formulate an optimization problem whose solution would give us the optimal mapping from the feature space, consisting of the time varying observed battery parameters to the label space, consisting of the state of charge. Note that in equation 2 we have parameterized f by θ . This significantly simplifies the problem of optimization in a functional space by converting it to a parameter optimization problem. However, to make it practically feasible for an optimizer to be able to find an acceptable value of θ with respect to generalization capability and error in estimation, we need to induce some reasonable biases on the parameter search space. Choosing a particular type of neural network architecture establishes this kind of an useful inductive bias on the parameter space. In our proposed method, a 1D convolutional neural network is used as f where θ represents its weights and biases such that $\theta \in \Theta_C$ where Θ_C refers to the CNN parameter space. We can now formulate an optimization problem as shown below:

$$\theta^* = \underset{\theta \in \Theta_C}{\operatorname{argmin}} G(|SOC_k - \widehat{SOC}_k|, \forall k = t_w, \dots, t_{end}) \quad (3)$$

where G is a distance function, taking as arguments, the absolute difference between the estimated and actual SOC values at each timestep. G can be a Mean Squared Error (MSE) function as shown in equation 4, a Mean Absolute Error function(MAE) as shown in equation 5 or a Maximum Absolute Error (MAX) function as shown in equation 6 . However G is not restricted to these functions only.

$$MSE = \frac{1}{L} \sum_{k=t_w}^{t_{end}} (|SOC_k - \widehat{SOC}_k|^2) \quad (4)$$

$$MAE = \frac{1}{L} \sum_{k=t_w}^{t_{end}} (|SOC_k - \widehat{SOC}_k|) \quad (5)$$

$$MAX = \max\{|SOC_k - \widehat{SOC}_k|, \forall k = t_w, \dots, t_{end}\} \quad (6)$$

where, $L = t_{end} - t_w + 1$

In this paper we use Mean Squared Error as the distance function for training the models. The Mean Absolute Error and the Maximum Absolute Error functions are used for comparing and validating the estimation algorithm. This optimization problem is solved using a gradient based Adam optimizer and backpropagation is used to update the weights of the neural network.

B. CNN for SOC Estimation

Convolutional Neural Networks are the state of the art deep learning algorithm for image processing. The performance of CNNs is attributed to three major features embedded within its architecture - local receptive fields, shared weights and subsampling. Invariably, a CNN consists of two main types of layers, a convolutional layer and a pooling layer. A typical

convolution layer of a 2D CNN is organised into planes of units, where each plane is known as a feature map. The units of a feature map are generated by convolving small subregions of the image with a filter or kernel. The filter corresponding to a particular feature map is constrained to have the same set of weights. This sharing of weights ensures that one feature map captures similar local features from different parts of the image. To account for multiple features, a convolutional layer thus consists of multiple filters giving rise to multiple feature maps. The output of the convolutional layer is then passed onto a pooling layer which performs the subsampling operation. The pooling layer consists of a plane of units corresponding to each feature map in the convolutional layer. Each unit is formed after performing a subsampling operation like an average or max operation over a small receptive field in the corresponding feature map of the convolutional layer.

Unlike in a 2D CNN, where the kernels or filters stride across both the spatial dimensions of an image, i.e., from left to right and from top to bottom, kernels in 1D CNNs stride only in one dimension, which is the temporal dimension in case of time series data and thus are able to extract local temporally relevant features.

For the purpose of SOC estimation, the proposed 1D CNN model takes the voltage, current and temperature values of a battery corresponding to timesteps $k - t_w$ to k as inputs and predicts the SOC value at timestep k . Throughout our experiments we fix t_w to be 500, where each timestep corresponds to 0.1 seconds. Two basic CNN architectures, namely the dense first and the merge first architectures were developed for this application. As shown in figures 1 and 2, the initial layers of the two architectures, consisting of convolutional and pooling layers are identical to each other. The first convolutional layer extracts three disjoint clusters of feature maps from the input. These clusters are formed by convoluting the input data sequence with three differently shaped filters or kernels of shapes 10×3 , 50×3 and 100×3 along the temporal axis. The first dimension of the filters corresponds to the number of datapoints along the time axis that are considered at once for convolution whereas the second dimension corresponds to the dimensionality of the feature space, which is 3, corresponding to battery voltage, current and temperature. The intention behind using filters of different shapes is to capture both long and short term temporal dependencies in the data and to extract appropriate features representing them in a single convolutional layer. The subsequent convolutional and pooling layers follow suit and maintain the clustered feature map appearance where each cluster of feature maps in one layer is derived from its corresponding predecessor in the previous layer. The shape of the filters in the subsequent convolutional and pooling layers were kept the same for each of the three feature map clusters in a given layer.

The difference in the architectures, however, is in terms of the positional arrangement of the final fully connected dense layers. In the merge first architecture, the feature maps extracted from the final pooling layer are concatenated after flattening and then given as input to the dense layer, whereas in the dense first architecture, the flattened feature maps are given as inputs to three disjoint fully connected dense layers

and no concatenation operation is performed. The final neuron gives the SOC estimate in both the cases.

C. Knowledge Transfer across datasets

Machine learning models are known to be notoriously task specific, i.e., if an ML model is trained from data sampled from a joint distribution $\mathbb{P}(X, Y)$ and the previously unseen test data is also sampled from the marginal corresponding to the same joint distribution, it provides accurate estimation results. However, if the test data is sampled from a marginal feature distribution corresponding to a different but related joint distribution $\mathbb{Q}(X, Y)$, the estimator performs poorly.

More formally, a machine learning problem can be characterized by a domain and a task. The domain comprises of the feature space \mathcal{X} and the marginal feature distribution $\mathbb{P}(X)$ while the task comprises of the label space \mathcal{Y} and the posterior of the labels conditioned on features, i.e., $\mathbb{P}(Y|X)$. A transfer learning task formally identifies a source domain \mathfrak{D}_s and a corresponding task \mathfrak{T}_s and a target domain \mathfrak{D}_t and a corresponding task \mathfrak{T}_t and aims at transferring knowledge across them.

Depending on what changes in the domain or the task when we shift from a source problem to a new target problem, transfer learning can be classified as inductive, transductive and unsupervised[5]. The SOC estimation problem across different battery types falls under the transductive class of transfer learning algorithms that are used when the source and target domains are different but related. More specifically, we assume that the feature spaces are the same but the marginal feature distribution are different, i.e., $X_s \neq X_t \Rightarrow \mathbb{P}_s(X) \neq \mathbb{P}_t(X)$ but the corresponding tasks are the same, i.e., $\mathfrak{T}_s = \mathfrak{T}_t$.

In order to establish the benefits of using transfer learning empirically, we use two publicly available battery datasets in this paper- Dataset A: Panasonic 18650 PF battery dataset , Dataset B: LG 18650 dataset. Details of the datasets are given in section III.

Considering the fact labelled data is available in case of both the source and target problems, a simple weight sharing algorithm is used for implementing transfer learning in our case. The weights of the 1D CNN model first trained on Dataset A(source data) is used as the initial set of weights for training an identical model on Dataset B(target data). Two separate modes of training are considered by freezing appropriate layer weights, the details of which have been elaborated in Section IV-C.

III. DATASET DESCRIPTION

Two publicly available LiB datasets have been used for experimentation in this paper, the detailed specifications of which can be found in [15] and [21].

A. Dataset A – Panasonic 18650 PF battery dataset

This dataset was prepared in the University of Wisconsin Madison [15]. The battery cell consists of a Lithium Nickel Cobalt Aluminum Oxide ($LiNiCoAlO_2$ or NCA) chemistry. The data collected in this dataset corresponds to

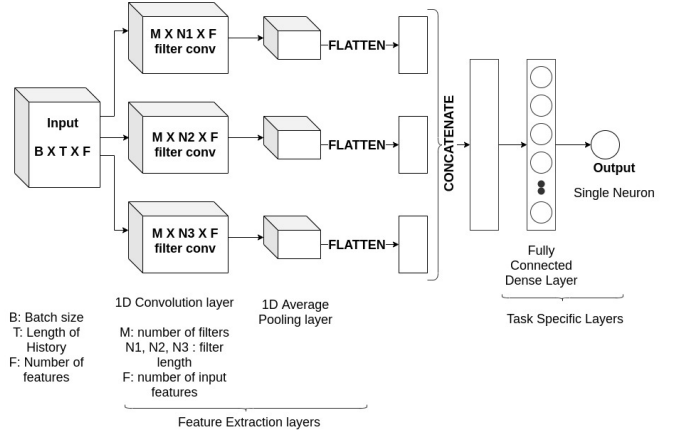


Fig. 1: Merge first architecture

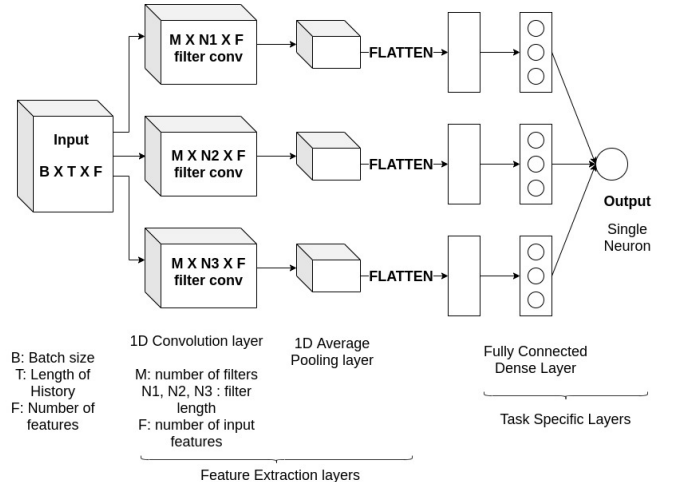


Fig. 2: Dense first architecture

tests conducted at different ambient temperatures ranging from -20°C to 25°C . For each test the battery cell was first fully charged and then a power drive cycle profile was executed on it. The drive cycles correspond to a Ford F150 truck and were drawn from the battery cell during discharge till the cell voltage reached its cut off value of 2.5V. The four standard drive cycles that the battery was put to test with were –Urban Dynamometer Driving Schedule (UDDS) , Highway Fuel Economy Driving Schedule (HWFET) , Los Angeles 92 (LA92) and Supplemental Federal Test Procedure Driving Schedule (US06). Some additional drive cycles were manually created for obtaining additional dynamics. These cycles, namely, Cycle 1, Cycle 2, Cycle 3, Cycle 4, and Neural Network (NN), consist of a random mix of UDDS, HWFET, US06 and LA92. Thus data corresponding to a total of 9 drive cycles are available. The charging dynamics are always the same. Data corresponding to Cycle 2 at an ambient temperature of 25°C is plotted in figure 3. The state of charge as can be seen has a highly non linear characteristic.

B. Dataset B – LG 18650 HG2 battery dataset

This dataset was prepared in the McMaster University, Ontario, Canada [21]. A 3Ah LG HG2 cell, with a Lithium

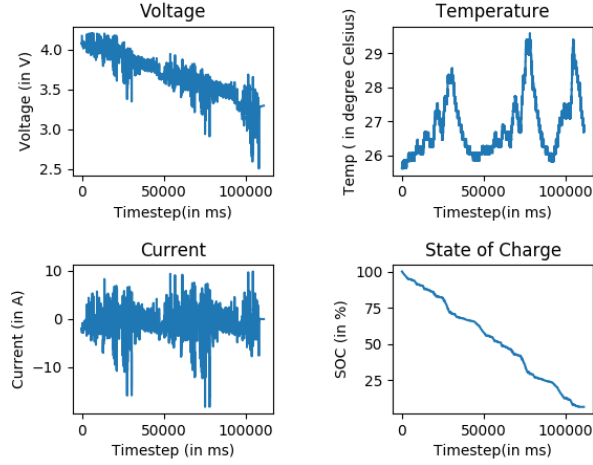


Fig. 3: Cycle 2 drive cycle data at 25°C from the Panasonic Dataset

Nickel Manganese Cobalt oxide ($Li[NiMnCo]O_2$ or NMC) chemistry, was put under a series of tests under six different ambient temperatures ranging from -20°C to 40°C . The tests conducted were similar to that on Dataset A. Four standard drive cycles were drawn from the battery – UDDS, LA92, HWFET and US06. Apart from these eight additional cycles were artificially created, namely, Mixed 1, Mixed 2, Mixed 3, Mixed 4, Mixed 5, Mixed 6, Mixed 7 and Mixed 8. These cycles are a random mix of the four standard drive cycles. The battery was fully charged before each test and was discharged through these drive cycle profiles till 95% of the 1C discharge capacity at the respective temperature was drawn from the cell. Figure 4 consists of the visual depiction of data corresponding to relevant battery parameters for Mixed 2 cycle at 25 °C.

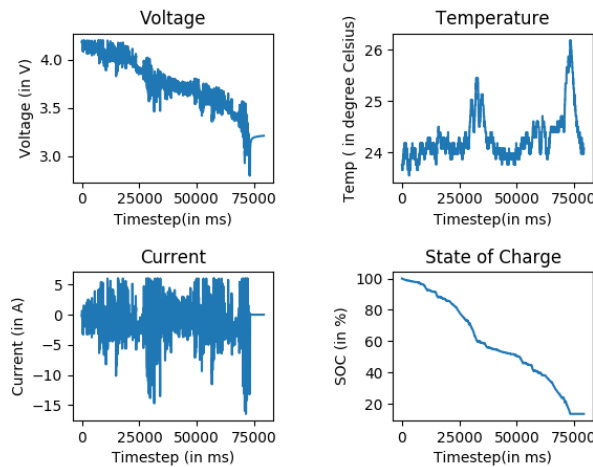


Fig. 4: Mixed 2 drive cycle data at 25°C from the LG 18650 HG2 Dataset

IV. EXPERIMENTAL SETUP

The experiments conducted for this paper can be broadly categorized into three subsequent sections as elaborated below.

A. Architecture Selection

These are the first set of experiments conducted in this paper. The aim of these experiments is to identify the best set of hyper-parameters suiting the concerned application. The best set of hyper-parameters identified from this are used to define the 1D CNN network architecture which is used in subsequent experiments. Here we focus specifically on the number of convolutional layers and the position of the fully connected dense layers as the concerned hyper-parameters for tuning. To consider the effect of varying the position and organization of the fully connected dense layers, the two architectures depicted in figures 1 and 2 are tested. For each of these two basic architectures the number of convolutional layers are varied between 1 and 2. Hence a total of four CNN architectures are tested in these set of experiments.

Seven drive cycles, namely, Cycle 1 to 4, UDDS and LA92 from Dataset A are considered for training a particular architecture of the model at different ambient temperatures individually. For each architecture under consideration, a model was independently trained on three different datasets, each consisting of the aforementioned seven drive cycles recorded at one of the three considered ambient temperatures - 0°C , 10°C and 25°C . After training, each architecture is evaluated on the remaining two drive cycles – US06 and HWFET - recorded at ambient temperatures corresponding to the dataset that they were trained with and the MAE and MAX errors of estimation were recorded. The model architecture which gives the least error in estimation under all the three ambient temperatures considered is used for further experiments. The entire architecture of the finally selected model is given in table I.

B. Model training and evaluation

This is the second set of experiments where we use the best architecture obtained from the first set of experiments for training and evaluation over a larger dataset obtained from Dataset A. The trained model obtained from this experiment will be the actual SoC estimator that can be deployed in an EV.

All the seven drive cycles used for the architecture selection experiments for three ambient temperatures 0°C , 10°C and 25°C were concatenated to a single dataset and used for training a model constituting of the best performing architecture obtained using the prior experiments. That model was evaluated on the remaining drive cycles at different ambient temperatures. Hence the training dataset consisted of 21 drive cycles and the test data set consisted of 6 drive cycles. The MAE and MAX errors were recorded and the final trained weights of the model were stored.

Training was carried out for 100 epochs in a mini-batch fashion with a batch size of 128 and a separate validation dataset was created by selecting three random drive cycles from the training data which was used to check the validation performance after every epoch. The training was stopped when validation error didn't decrease for 10 consecutive epochs and the model weights giving the best validation performance were selected for evaluation.

TABLE I: Architecture of the best performing model obtained from the architecture selection experiment

Hyperparameters	Values
Number of convolutional layers	2
Architecture Type	Dense First
Number of neurons in each individual dense layer cluster in the penultimate layer	64
Shapes of filters in 1st convolutional layer	10, 50 and 100
Number of filters of each type in the 1st conv layer	16
Shapes of filters in 2nd convolutional layer	10, 10 and 10
Number of filters of each type in the 2nd conv layer	8
Number of pooling layers	1
Position of pooling layer	After the 2nd convolutional layer
Type of pooling	Average Pooling
Shapes of pooling filters	10, 10 and 10
Activation used in other than final layer	Leaky ReLu
Activation used in final layer	ReLu
Regularizer	L2 with coeff of 1e-4 (in the final layer)
Dropout probability	0.01

C. Transfer learning on different dataset

These are the final set of experiments performed in this paper, demonstrating a transfer learning scheme to improve the performance of the SoC estimator obtained from the second set of experiments, when applied over Dataset B.

The final weights of the model trained on Dataset A, i.e., the source data, in the previous experiment were used to initialize the weights of an identical model to be trained on Dataset B, i.e., the target data. The training data for this experiment consisted of 45 drive cycles – nine drive cycles corresponding to each of the four ambient temperatures considered from dataset B - -10°C , 0°C , 10°C , 25°C and 40°C . The nine drive cycles considered for each ambient temperature were randomly selected without replacement. From amongst the remaining drive cycles not selected into the training data, one dataset from each ambient temperature was selected at random to form a validation dataset and one more randomly selected drive cycle from each ambient temperature was used for evaluating the model. So the validation and test datasets each had five randomly selected drive cycles. Two different transfer learning scenarios were considered which are elaborated as follows:

1) Transfer Learning Scenario 1:

All the weights of the model to be trained on dataset B were allowed to be modified during the training procedure.

2) Transfer Learning Scenario 2:

All the weights corresponding to the fully connected layers of the model were frozen following initialization. Only the convolutional layers' weights were allowed to change during training on Dataset B.

The intuition behind training just the initial layers of the

CNN model in Transfer Learning Scenario 2 arises from the fact that the initial layers perform the function of feature selection and since the source and target domains are different the features selected for the task corresponding to the target domain need to be different than those used for the source task.

Training was carried out for a maximum of 100 epochs in the mini-batch fashion with a batch size of 128 and early stopping was implemented based on validation error.

For comparison purposes, as a baseline, a randomly initialized model, identical in architecture to the ones trained in this set of experiments, was also trained on the same training dataset derived from Dataset B, following a similar training procedure with early stopping. Hereafter we refer to this as the baseline model and it represents the case where we start training a deep learning model from scratch when we get a new and different dataset.

V. RESULTS AND DISCUSSIONS

The following section consists of the results of the various experiments described in the previous section and subsequent inferences from the observed results.

A. Architecture Selection

The final results comprising of MAE and MAX errors corresponding to each of the tested architectures and measured on the test datasets at each temperature are given in Table II.

As can be observed the dense first architecture with two convolutional layers performs reasonably better than the other architectures and gives a minimum MAE error of 0.58% and a MAX error of 2.78% at 25°C . A possible explanation for this could be that appropriately stacked convolutional layers are able to extract complex underlying features relevant to SOC estimation while discarding unwanted information. In the remaining part of the paper we shall refer to this architecture as the $2C - DF$ architecture. We will also use only the $2C - DF$ architecture for further experimentation. Notably, the performance of all the other architectures are also appreciable and all of them provide MAE errors of less than 2%.

B. Model Evaluation

The $2C - DF$ architecture model is trained on the 21 drive cycle dataset as described in section IV-B. The MAE and MAX estimation errors evaluated on the testing data is given in Table III. Figure 6 shows the estimated SOC vs actual SOC for the US06 drive cycle at 25°C .

The MSE losses obtained during training and validation have been depicted as a function of the number of epochs in figure 5. As can be seen from the figure training loss converges very fast. The training was continued even after convergence of the training loss to allow for a decrease in the validation loss. 100 epochs has been found to be more than sufficient for the training purpose.

Compared to the estimators proposed or mentioned in [13], [12], [17] and [22], our proposed estimator gives lesser or atleast equal estimation error measured on the same dataset.

TABLE II: Estimation error for the architecture selection experiment. The errors under each drive cycle is in the form MAE (%) / MAX(%)

Architecture type	Number of convolutional layers	Temperature (in degree Celsius)					
		0		10		25	
		US06	HWFET	US06	HWFET	US06	HWFET
Merge first	1	0.98/4.27	1.33/3.61	0.76/3.41	1.18/5.23	0.89/3.87	0.99/4.26
Merge first	2	1.18/7.55	1.59/3.98	0.64/4.96	1.16/5.23	0.75/2.9	0.89/4.21
Dense first	1	0.91/5.12	1.34/3.93	0.82/6.1	1.26/4.66	0.96/3.68	1.123/4.42
Dense first	2	1.25/6.5	1.62/3.66	0.85/3.5	1.13/5.09	0.58/2.78	0.77/4.33

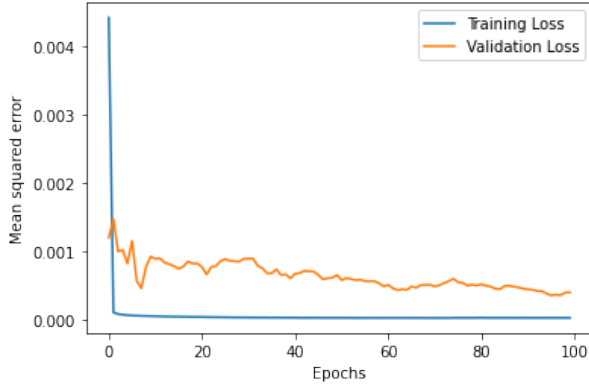


Fig. 5: Training and Validation loss vs Epochs on Dataset A.

Moreover the number of epochs required for training the LSTM model in [12] and the GRU model in [17] is considerably higher and in the range of a few thousands.

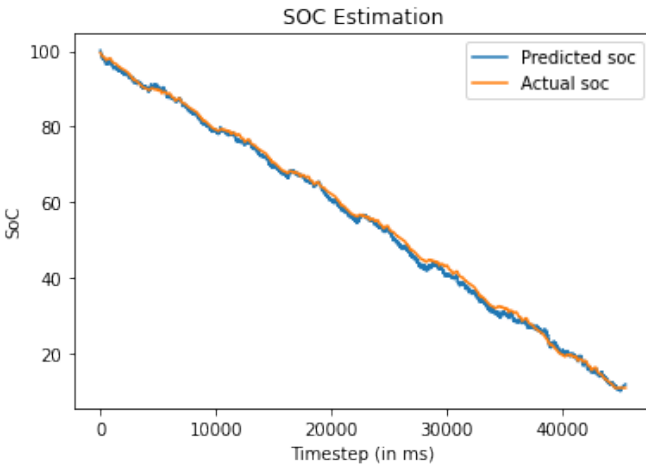


Fig. 6: SOC estimation on US06 drive cycle of Dataset A using a 2 layer dense first architecture.

C. Transfer learning on different dataset

A model with $2C - DF$ architecture is initialized with the final trained weights of the $2C - DF$ model trained on Dataset A in the prior experiment. Following which the new model is trained on Dataset B following the transfer learning scenarios

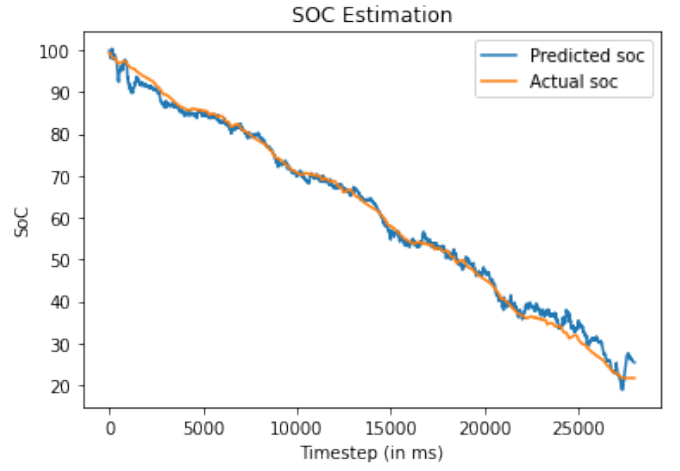


Fig. 7: SOC estimation on test data at 0°C from Dataset B using the baseline randomly initialized model.

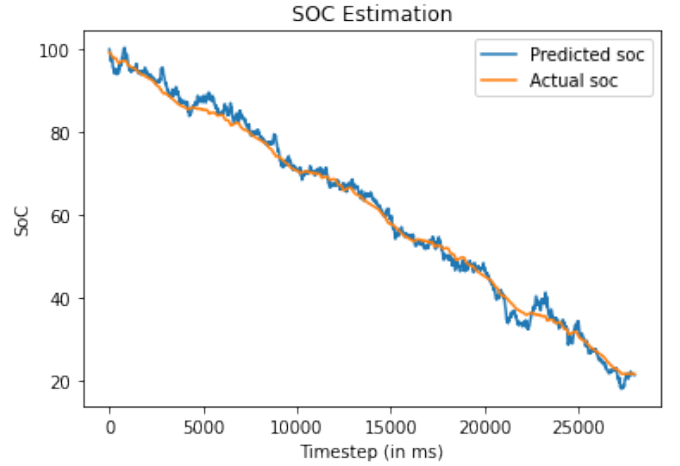


Fig. 8: SOC estimation on test data at 0°C from Dataset B using the model corresponding to the transfer learning scenario 1 where all the weights of the model was retrained.

described in section IV-C. Also a randomly initialized baseline model was trained on Dataset B for comparison purposes. The MAE and MAX errors obtained on the test dataset for all the considered scenarios are shown in Table IV. Also, figures 7, 8 and 9 plot the estimated and real SOC values as a function

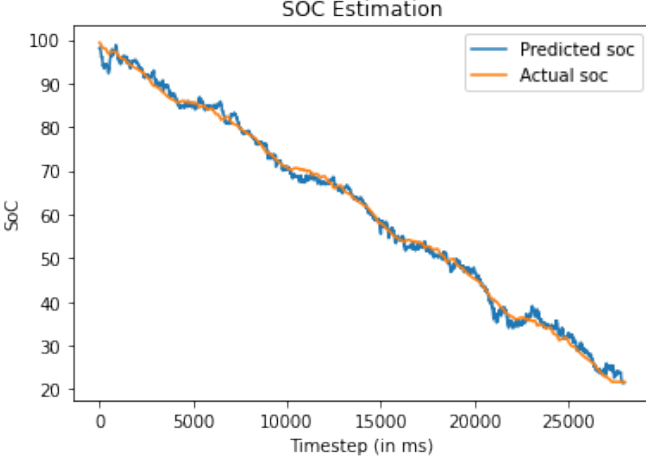


Fig. 9: SOC estimation on test data at 0°C from Dataset B using the model corresponding to the transfer learning scenario 2 where only the convolutional layer weights were retrained.

TABLE III: Estimation error values obtained on the test datasets derived from Dataset A for the $2C - DF$ architecture based model.

Ambient Temperature (degree Celsius)	MAE (in %)		MAX (in %)	
	US06	HWFET	US06	HWFET
0	1.66	0.86	6.21	4.3
10	1.63	1.63	5.25	6.81
25	0.85	1.21	2.83	4.45

of time for the test dataset at 0°C for all the three cases given in Table IV.

TABLE IV: Estimation errors recorded on the test dataset derived from Dataset B for the two transfer learning scenarios and the baseline model. TL1 represent the transfer learning scenario 1 while TL2 represents transfer learning scenario 2.

Temp	Baseline		TL 1		TL 2	
	MAE(%)	MAX(%)	MAE(%)	MAX(%)	MAE(%)	MAX(%)
-10	1.34	4.98	2.02	8.24	1.27	6.73
0	1.28	5.9	1.37	6.05	1.07	4.8
10	1.18	4.98	1.47	5.29	1.31	5.4
25	1.69	5.58	1.8	6.54	1.79	5.58
40	1.56	6.7	1.8	7	1.72	7.8

The transfer learning models perform at par in terms of estimation accuracy with the baseline model. At 0°C, the MAE in SoC estimation obtained for the baseline, transfer learning scenario 1 and transfer scenario 2 models are 1.28%, 1.47% and 1.07% respectively. This shows that with the intelligent weight initialization, retraining only a few weights is sufficient to achieve an estimation accuracy which is at par with what can be achieved with a randomly initialized model trained completely on the new dataset.

The training error as a function of the number of epochs has been plotted in figure 10 for the baseline model and

transfer learning scenario 2. It can be observed that with transfer learning the value of the training loss starts to increase after around 50 epochs. So the transfer learning model attains minimum training error at around half the number of epochs required to train an equivalent model from scratch without transfer learning.

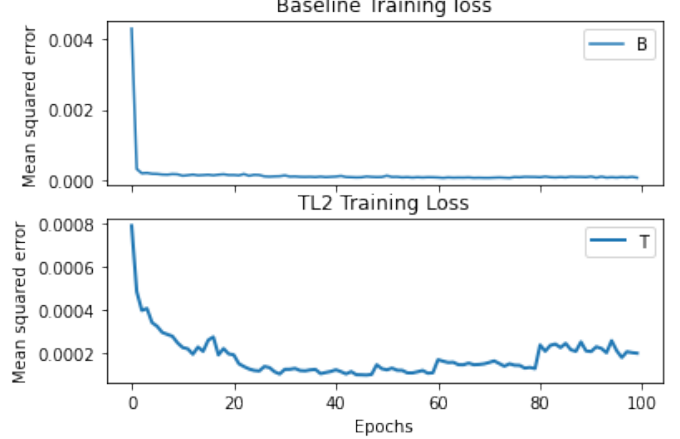


Fig. 10: (top)Training loss vs epochs corresponding to the baseline model; (bottom)Training loss vs epochs corresponding to the transfer learning scenario 2

VI. CONCLUSION

Leveraging 1D convolutional neural networks and transfer learning, a novel SOC estimation algorithm has been proposed in this paper. The convolutional neural network learns the underlying features form the time series battery data and estimates the SOC at a given timestep. Different architectures were tested and a 2 convolutional layer dense first type model was found to be the best performing network in the proposed experimental setup. The estimation error obtained from the selected architecture is found to be better than or at par with the state of the art machine learning algorithms used for SOC estimation. Using a transfer learning framework, the generalizability of the model is improved and the training time is found to have reduced. Further implications of implementing a transfer learning framework lies in its merit that whenever a new battery is encountered, only a few weights of the existing SOC estimation model require re-training and that too for a considerably shorter amount of time.

REFERENCES

- [1] S. Rodrigues, N. Munichandraiah, and A. Shukla, “A review of state-of-charge indication of batteries by means of a.c. impedance measurements,” *Journal of Power Sources*, vol. 87, no. 1, pp. 12–20, 2000, ISSN: 0378-7753. DOI: [https://doi.org/10.1016/S0378-7753\(99\)00351-1](https://doi.org/10.1016/S0378-7753(99)00351-1).
- [2] G. L. Plett, “Extended kalman filtering for battery management systems of lipb-based hev battery packs: Part 3. state and parameter estimation,” *Journal of Power Sources*, vol. 134, no. 2, pp. 277–292, 2004, ISSN: 0378-7753. DOI: <https://doi.org/10.1016/j.jpowsour.2004.02.033>.

[3] D. Lee, S. Shiah, C. Lee, and Y. Wang, "State-of-charge estimation for electric scooters by using learning mechanisms," *IEEE Transactions on Vehicular Technology*, vol. 56, no. 2, pp. 544–556, 2007.

[4] V. Pop, H. Bergveld, D. Danilov, P. Notten, and P. Regtien, *Battery management systems : accurate state-of-charge indication for battery-powered applications*, ser. Philips research book series. Germany: Springer, 2008, ISBN: 978-1-4020-6944-4. DOI: 10.1007/978-1-4020-6945-1.

[5] S. J. Pan and Q. Yang, "A survey on transfer learning," *IEEE Transactions on Knowledge and Data Engineering*, vol. 22, no. 10, pp. 1345–1359, 2010.

[6] K. W. E. Cheng, B. P. Divakar, H. Wu, K. Ding, and H. F. Ho, "Battery-management system (bms) and soc development for electrical vehicles," *IEEE Transactions on Vehicular Technology*, vol. 60, no. 1, pp. 76–88, 2011.

[7] H. He, R. Xiong, X. Zhang, F. Sun, and J. Fan, "State-of-charge estimation of the lithium-ion battery using an adaptive extended kalman filter based on an improved thevenin model," *IEEE Transactions on Vehicular Technology*, vol. 60, no. 4, pp. 1461–1469, 2011.

[8] R. Xiong, H. He, F. Sun, and K. Zhao, "Evaluation on state of charge estimation of batteries with adaptive extended kalman filter by experiment approach," *IEEE Transactions on Vehicular Technology*, vol. 62, no. 1, pp. 108–117, 2013.

[9] X. Chen, W. Shen, M. Dai, Z. Cao, J. Jin, and A. Kapoor, "Robust adaptive sliding-mode observer using rbf neural network for lithium-ion battery state of charge estimation in electric vehicles," *IEEE Transactions on Vehicular Technology*, vol. 65, no. 4, pp. 1936–1947, 2016.

[10] H. Chaoui and C. C. Ibe-Ekeocha, "State of charge and state of health estimation for lithium batteries using recurrent neural networks," *IEEE Transactions on Vehicular Technology*, vol. 66, no. 10, pp. 8773–8783, 2017.

[11] J. Yang, B. Xia, Y. Shang, W. Huang, and C. C. Mi, "Adaptive state-of-charge estimation based on a split battery model for electric vehicle applications," *IEEE Transactions on Vehicular Technology*, vol. 66, no. 12, pp. 10 889–10 898, 2017.

[12] E. Chemali, P. J. Kollmeyer, M. Preindl, R. Ahmed, and A. Emadi, "Long short-term memory networks for accurate state-of-charge estimation of li-ion batteries," *IEEE Transactions on Industrial Electronics*, vol. 65, no. 8, pp. 6730–6739, 2018.

[13] E. Chemali, P. J. Kollmeyer, M. Preindl, and A. Emadi, "State-of-charge estimation of li-ion batteries using deep neural networks: A machine learning approach," *Journal of Power Sources*, vol. 400, pp. 242–255, 2018, ISSN: 0378-7753. DOI: <https://doi.org/10.1016/j.jpowsour.2018.06.104>.

[14] M. A. Hannan, M. S. H. Lipu, A. Hussain, M. H. Saad, and A. Ayob, "Neural network approach for estimating state of charge of lithium-ion battery using backtracking search algorithm," *IEEE Access*, vol. 6, pp. 10 069–10 079, 2018.

[15] P. Kollmeyer, "Panasonic 18650pf li-ion battery data," *Mendeley Data*, vol. 1, 2018. DOI: 10.17632/wykht8y7tg.1.

[16] A. C. Caliwag and W. Lim, "Hybrid varma and lstm method for lithium-ion battery state-of-charge and output voltage forecasting in electric motorcycle applications," *IEEE Access*, vol. 7, pp. 59 680–59 689, 2019.

[17] C. Li, F. Xiao, and Y. Fan, "An approach to state of charge estimation of lithium-ion batteries based on recurrent neural networks with gated recurrent unit," *Energies*, vol. 12, no. 9, p. 1592, Apr. 2019, ISSN: 1996-1073. DOI: 10.3390/en12091592.

[18] X. Song, F. Yang, D. Wang, and K. Tsui, "Combined cnn-lstm network for state-of-charge estimation of lithium-ion batteries," *IEEE Access*, vol. 7, pp. 88 894–88 902, 2019.

[19] C. Vidal, P. Kollmeyer, E. Chemali, and A. Emadi, "Li-ion battery state of charge estimation using long short-term memory recurrent neural network with transfer learning," in *2019 IEEE Transportation Electrification Conference and Expo (ITEC)*, 2019, pp. 1–6.

[20] B. Xiao, Y. Liu, and B. Xiao, "Accurate state-of-charge estimation approach for lithium-ion batteries by gated recurrent unit with ensemble optimizer," *IEEE Access*, vol. 7, pp. 54 192–54 202, 2019.

[21] P. Kollmeyer, C. Vidal, M. Naguib, and M. Skells, "Lg 18650hg2 li-ion battery data and example deep neural network xev soc estimator script," *Mendeley Data*, vol. 3, 2020. DOI: 10.17632/cp3473x7xv.3.

[22] C. Vidal, P. Malysz, P. Kollmeyer, and A. Emadi, "Machine learning applied to electrified vehicle battery state of charge and state of health estimation: State-of-the-art," *IEEE Access*, vol. 8, pp. 52 796–52 814, 2020.